Science Advances
AAAS

Supplementary Materials for

Tripartite extended amygdala–basal ganglia CRH circuit drives locomotor activation and avoidance behavior

Simon Chang *et al.*

Corresponding author: Jan M. Deussing, deussing@psych.mpg.de

Sci. Adv. **8**, eabo1023 (2022)
DOI: 10.1126/sciadv.abo1023

The PDF file includes:

Figs. S1 to S13
Legends for movies S1 to S5

Other Supplementary Material for this manuscript includes the following:

Movies S1 to S5

Figures

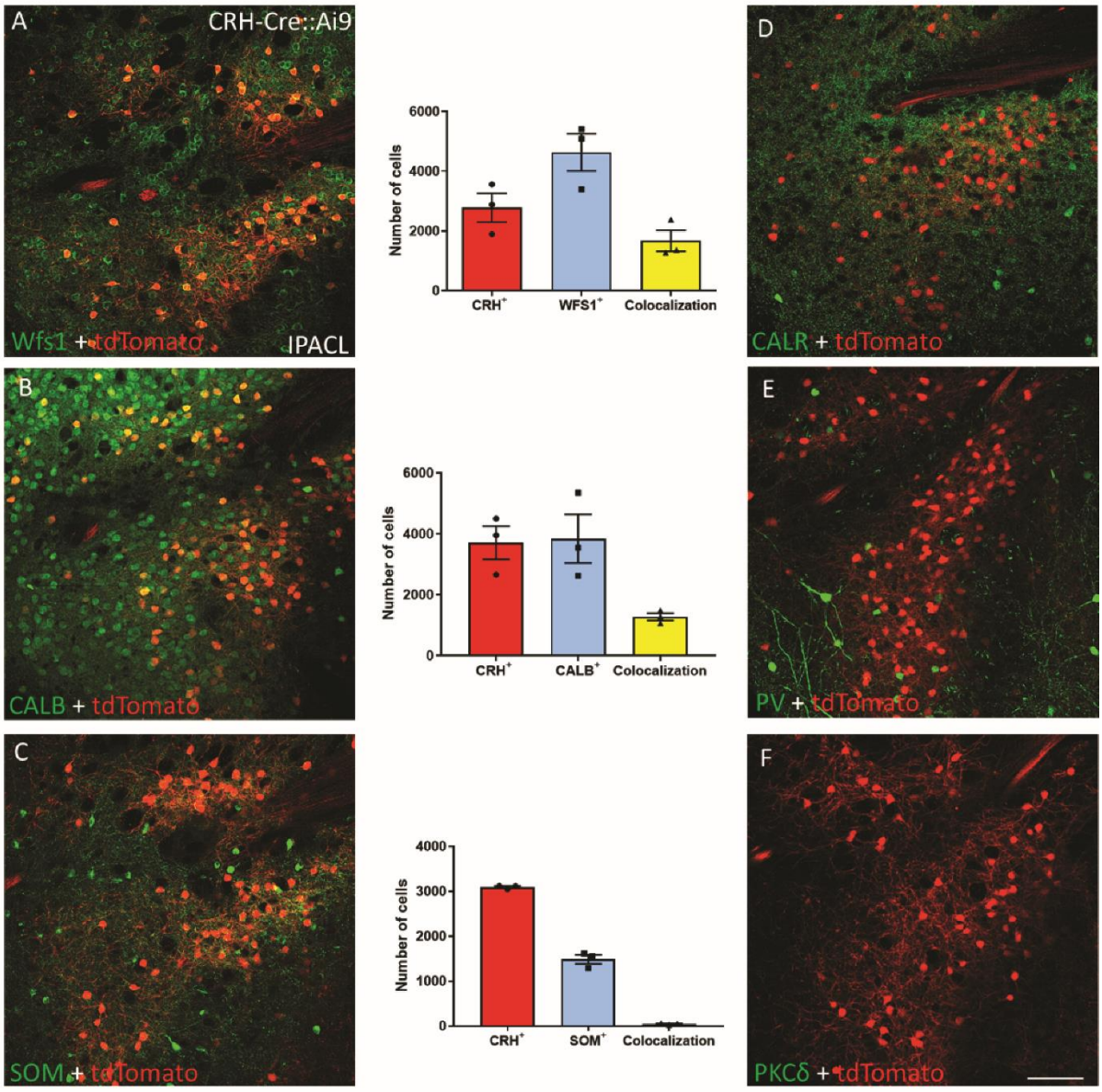

Figure S1. Characterization of CRH neurons in the extended amygdala. (**A-F**) Representative images of IPACL^{CRH} neurons co-stained with markers of GABAergic neurons and (**A-C**) quantification of co-localization. Abbreviations: CALB, calbindin; CALR, calretinin; PKCδ, protein kinase Cδ; PV, parvalbumin; SOM, somatostatin; WFS1, wolframin ER transmembrane glycoprotein 1. Values represent mean ± SEM, scale bar = 200 µm.

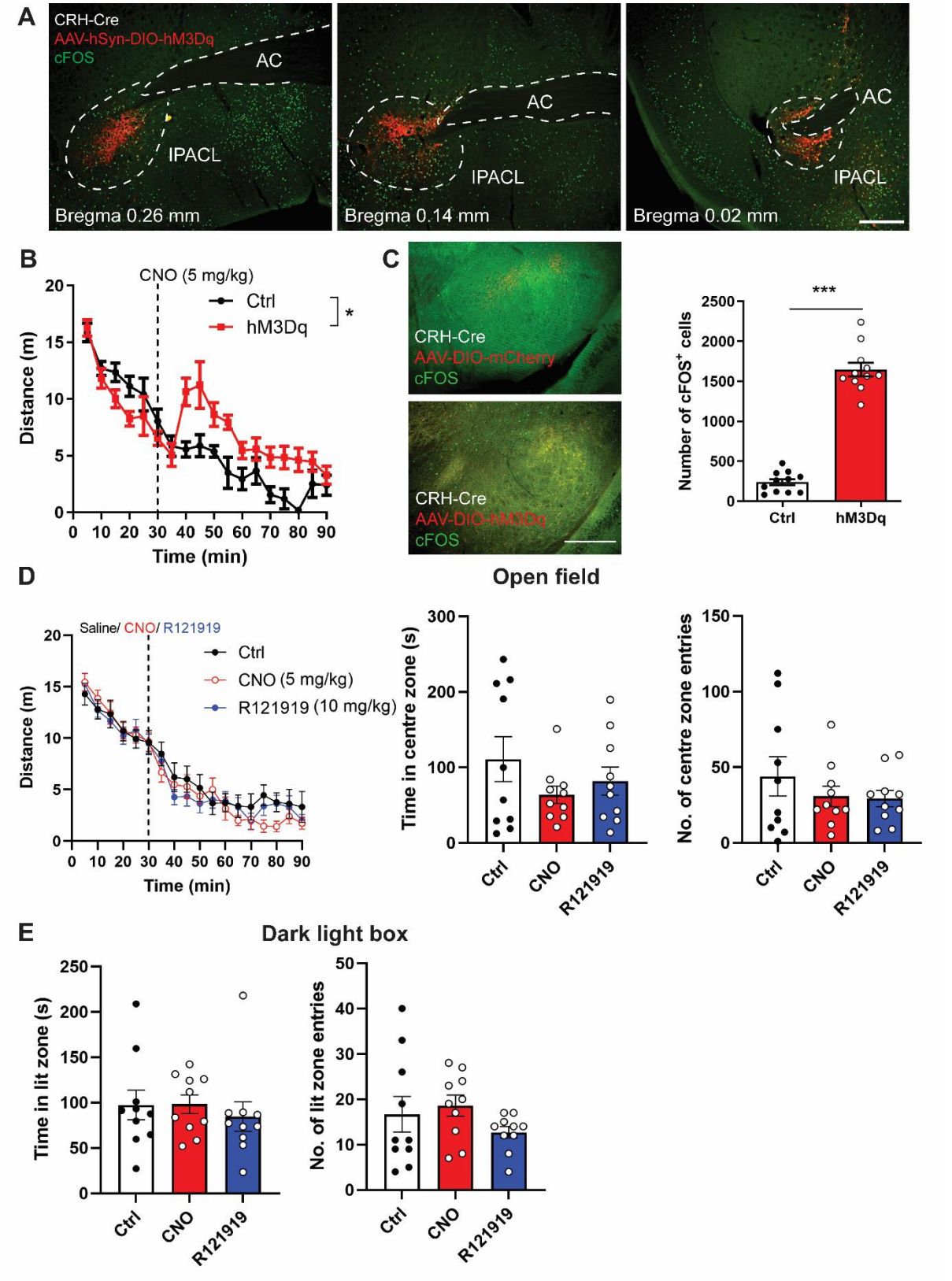

Figure S2. Assessing consequences of chemogenetic activation of IPACL^{CRH} neurons and respective control conditions. (**A)** Representative images of coronal brain sections of CRH-Cre animals injected with AAV$_8$-hSyn-DIO-hM3Dq-mCherry (hM3Dq) in the IPACL and

stained for cFOS following CNO administration, scale bar = 200 µm. (**B**) Distance CRH-Cre mice expressing hM3Dq in the IPACL travelled in a 90-min OF with CNO administration at 30 min (n = 10 animals per group; repeated measures two-way ANOVA, $F_{1,7} = 6.28$, $p = 0.04$). (**C**) Quantification of $cFOS^{+}$ cells in the SN ($p < 0.0001$, t = 14.92) 90 min following CNO administration in mice expressing hM3Dq in $IPACL^{CRH}$ neurons. (**D, E**) Control experiment testing for unspecific effects of CNO and R121919. (**D**) Distance travelled, time in centre zone and entries into centre (n = 10 animals per group). (**E)** Time in lit zone and entries into lit zone of the DaLi (n = 10 animals per group). Values represent mean ± SEM, * $p < 0.05$, ** $p < 0.01$, *** $p < 0.0001$.

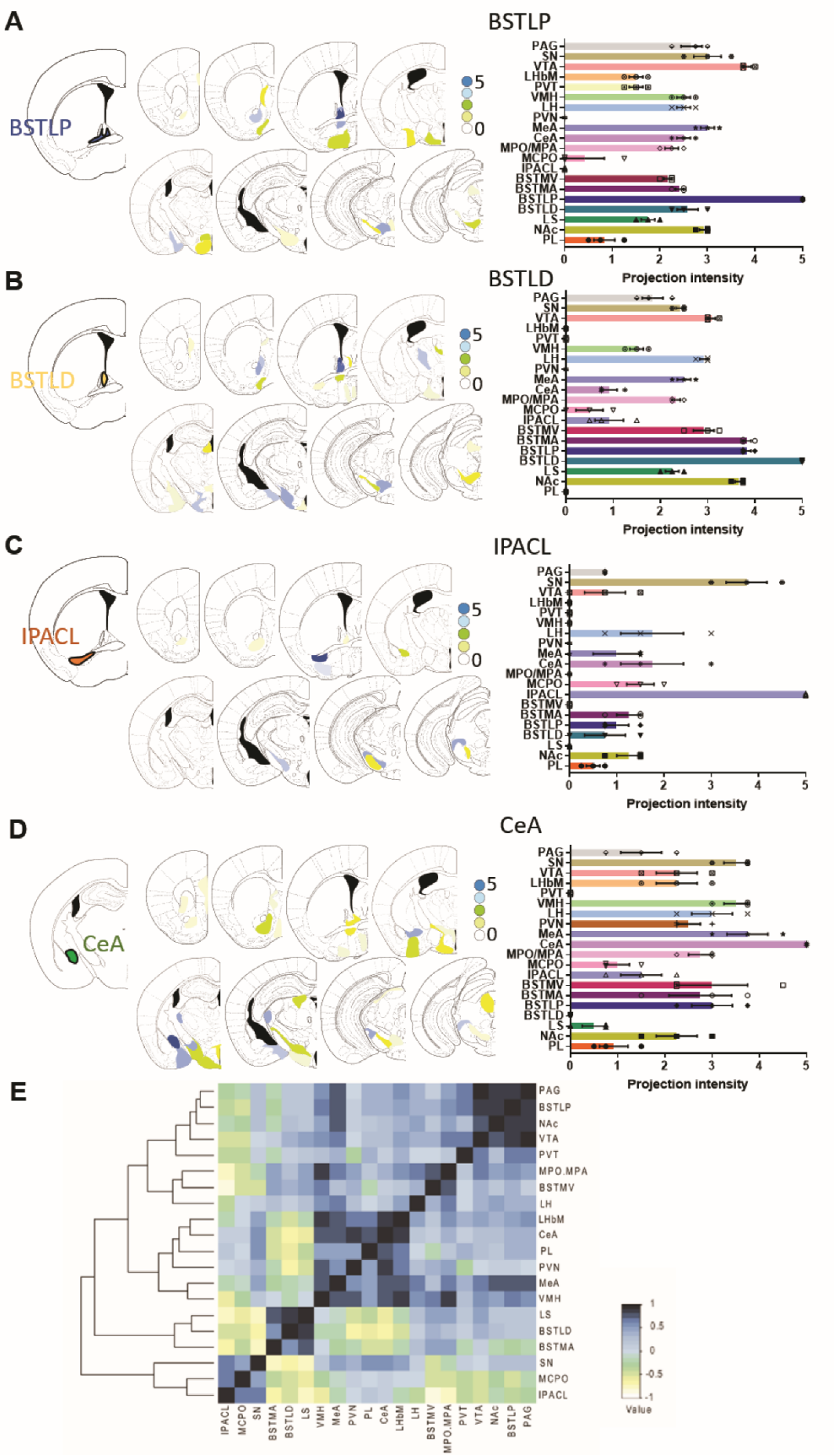
A
BSTLP
5
0
BSTLP
PAG
SN
VTA
LHbM
PVT
VMH
LH
PVN
MeA
CeA
MPO/MPA
MCPO
IPACL
BSTMV
BSTMA
BSTLP
BSTLD
LS
NAc
PL
0 1 2 3 4 5
Projection intensity
B
BSTLD
5
0
BSTLD
PAG
SN
VTA
LHbM
PVT
VMH
LH
PVN
MeA
CeA
MPO/MPA
MCPO
IPACL
BSTMV
BSTMA
BSTLP
BSTLD
LS
NAc
PL
0 1 2 3 4 5
Projection intensity
C
IPACL
5
0
IPACL
PAG
SN
VTA
LHbM
PVT
VMH
LH
PVN
MeA
CeA
MPO/MPA
MCPO
IPACL
BSTMV
BSTMA
BSTLP
BSTLD
LS
NAc
PL
0 1 2 3 4 5
Projection intensity
D
CeA
5
0
CeA
PAG
SN
VTA
LHbM
PVT
VMH
LH
PVN
MeA
CeA
MPO/MPA
MCPO
IPACL
BSTMV
BSTMA
BSTLP
BSTLD
LS
NAc
PL
0 1 2 3 4 5
Projection intensity
E
PAG
BSTLP
NAc
VTA
PVT
MPO.MPA
BSTMV
LH
LHbM
CeA
PL
PVN
MeA
VMH
LS
BSTLD
BSTMA
SN
MCPO
IPACL
IPACL MCPO SN BSTMA BSTLD LS VMH MeA PVN PL CeA LHbM LH BSTMV MPO.MPA PVT VTA NAc BSTLP PAG
1
0.5
0
-0.5
-1
Value

Figure S3. Anterograde tracing reveals target sites of CRH neurons of the extended amygdala. (**A-E**) Schematic illustration of injection sites of AAV_9-CMV-DIO-Syp-GFP within extended amygdala subdivisions in CRH-Cre mice. Summary of targets and strength of projections of CRH neurons located in the (A) BSTLP, (B) BSTLD, (C) IPACL and (D) CeA. (**E**) Pearson correlation demonstrating connectivity of brain regions based on anterograde tracing of CRH neurons. Abbreviations: BSTLD, bed nucleus of the stria terminalis, laterodorsal; BSTLP, bed nucleus of the stria terminalis, lateroposterior; BSTMA, bed nucleus of the stria terminalis, medial, anterior; BSTMV, bed nucleus of the stria terminalis, medial, ventral; LH/VMH, lateral hypothalamus/ventromedial hypothalamus; LHbM, lateral habenula, medial; LS, lateral septal nucleus; MCPO, magnocellular preoptic area; MeA, medial amygdaloid nucleus; MPO, median preoptic area; NAc, nucleus accumbens; PAG, periaqueductal grey; PL, prelimbic cortex; PVN, paraventricular nucleus of the hypothalamus; PVT, paraventricular thalamic nucleus.

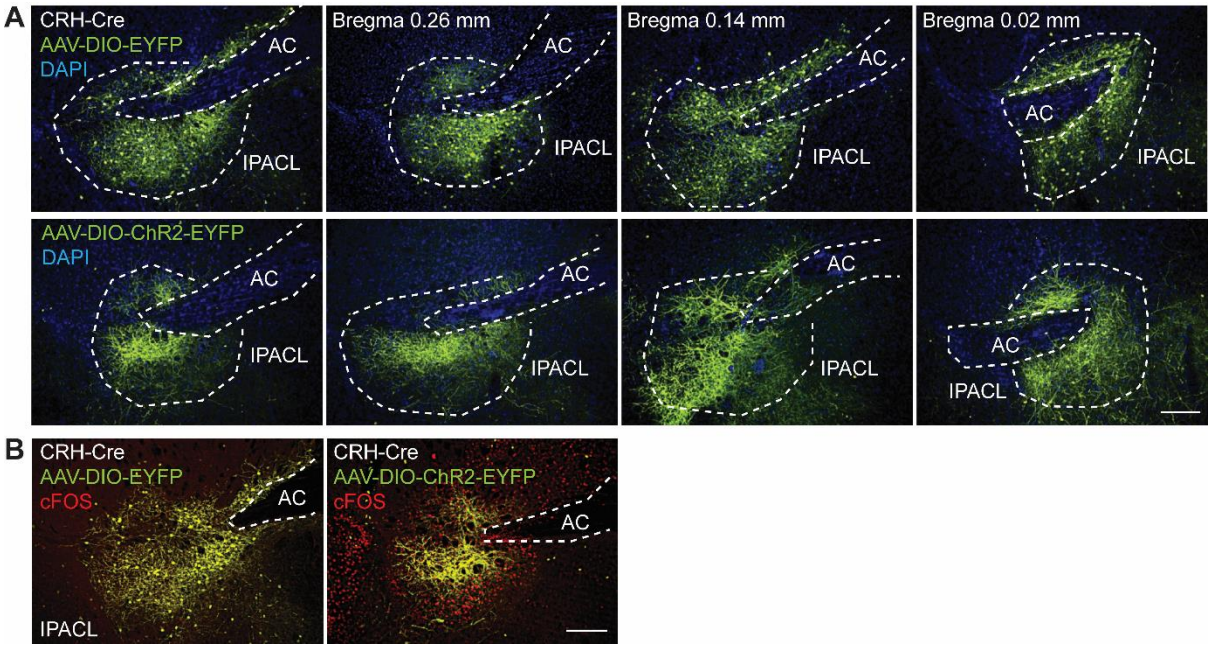

Figure S4. Optogenetic activation of IPACL^{CRH} neurons. (**A**) Representative images of coronal brain sections of CRH-Cre animals injected with AAV$_5$-Ef1a-DIO-ChR2-EYFP (ChR2) and AAV$_5$-Ef1a-DIO-EYFP (Ctrl) in the IPACL. (**B**) Representative images of coronal IPACL sections stained for cFOS (90 min after light on), scale bar = 200 µm.

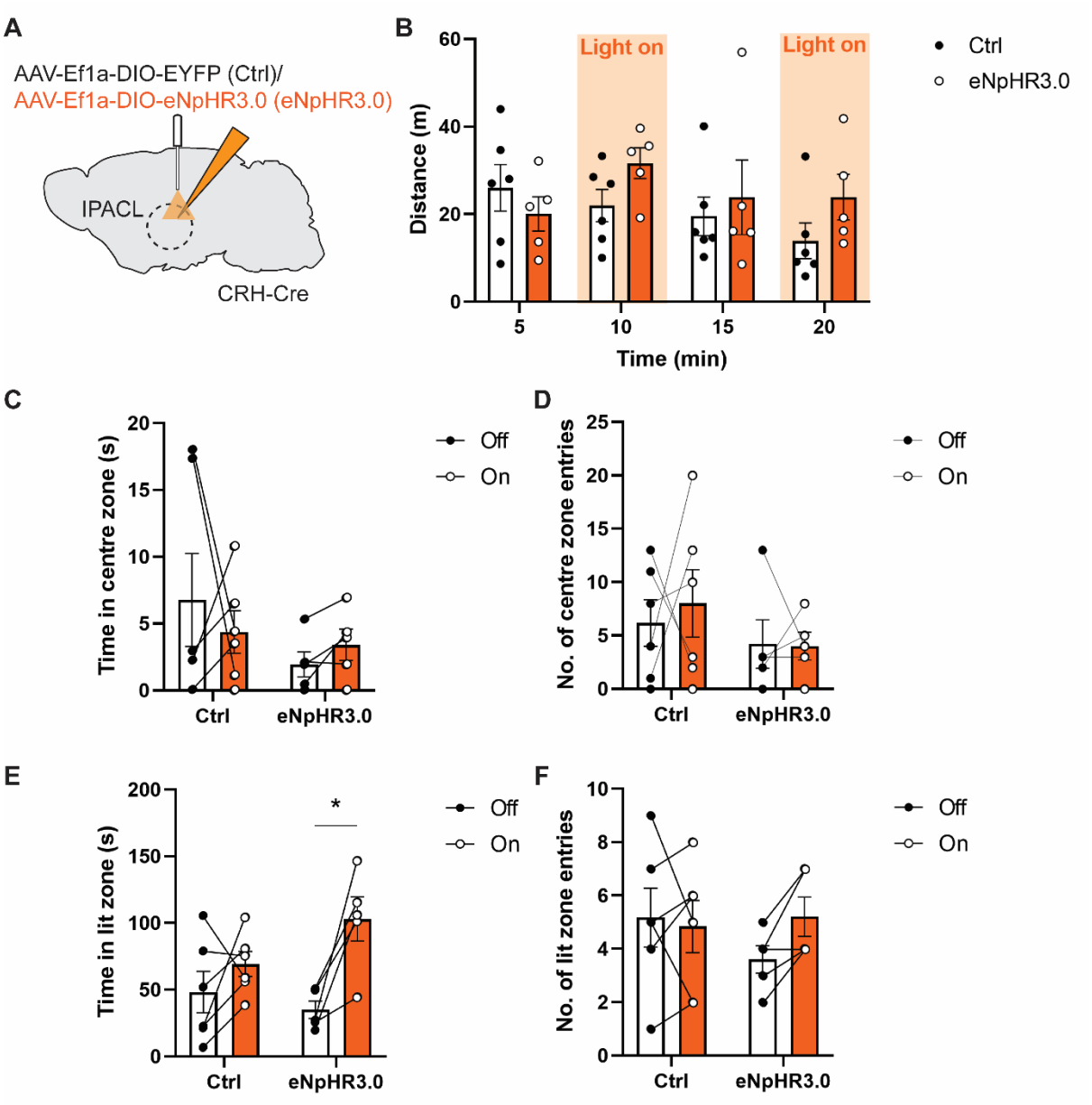

Figure S5. Optogenetic inhibition of IPACL^{CRH} neurons. (**A**) AAV_5-Ef1a-DIO-eNpHR3.0-EYFP (eNpHR3.0) or AAV_5-Ef1a-DIO-EYFP (Ctrl) into the IPACL and placement of optic fibre in the IPACL of CRH-Cre mice. (**B-F**) Inhibition of IPACL^{CRH} neurons did not alter behaviors in the OF or DaLi. (**B**) Distance travelled in OF with two 5-min light-induced inhibition sessions (n = 6 (Ctrl), n = 5 (eNpHR3.0); repeated measures two-way ANOVA, $F_{1,9}$ = 0.88, p = 0.37). (**C**) Time spent in centre (two-way ANOVA, $F_{1,18}$ = 1.69, p = 0.21) and (**D**) transitions into the centre zone (two-way ANOVA, $F_{1,18}$ = 1.51, p = 0.23) of the open field. (**E**) Time spent in lit zone (two-way ANOVA, Bonferroni's multiple comparison test, p = 0.01, t =

3.57) and (**F**) entries into lit zone (two-way ANOVA, $F_{1,18} = 0.43$, $p = 0.51$) of the dark-light box. Values represent mean ± SEM, * $p < 0.05$.

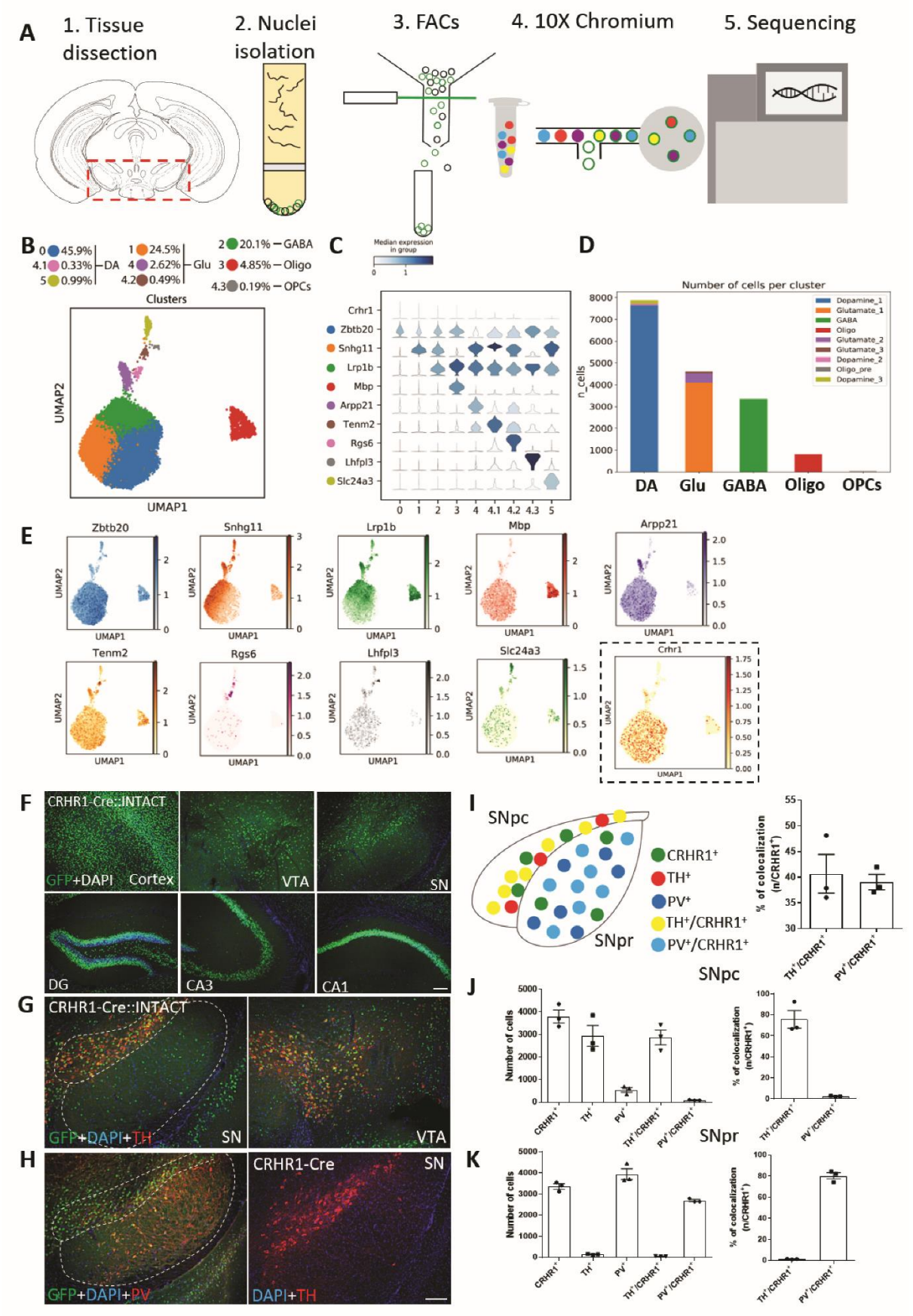
A
1. Tissue dissection
2. Nuclei isolation
3. FACs
4. 10X Chromium
5. Sequencing
B
0 45.9%
4.1 0.33%
5 0.99%
DA
1 24.5%
4 2.62%
4.2 0.49%
Glu
2 20.1% – GABA
3 4.85% – Oligo
4.3 0.19% – OPCs
Clusters
UMAP2
UMAP1
C
Median expression in group
Crhr1
Zbtb20
Snhg11
Lrp1b
Mbp
Arpp21
Tenm2
Rgs6
Lhfpl3
Slc24a3
0 1 2 3 4 4.1 4.2 4.3 5
D
Number of cells per cluster
n_cells
Dopamine_1
Glutamate_1
GABA
Oligo
Glutamate_2
Glutamate_3
Dopamine_2
Oligo_pre
Dopamine_3
DA
Glu
GABA
Oligo
OPCs
E
Zbtb20
Snhg11
Lrp1b
Mbp
Arpp21
Tenm2
Rgs6
Lhfpl3
Slc24a3
Crhr1
UMAP1
UMAP2
F
CRHR1-Cre::INTACT
GFP+DAPI
Cortex
VTA
SN
DG
CA3
CA1
G
CRHR1-Cre::INTACT
GFP+DAPI+TH
SN
VTA
H
GFP+DAPI+PV
CRHR1-Cre
SN
DAPI+TH
I
SNpc
SNpr
CRHR1+
TH+
PV+
TH+/CRHR1+
PV+/CRHR1+
% of colocalization (n/CRHR1+)
TH+/CRHR1+
PV+/CRHR1+
J
SNpc
Number of cells
% of colocalization (n/CRHR1+)
CRHR1+
TH+
PV+
TH+/CRHR1+
PV+/CRHR1+
K
SNpr
Number of cells
% of colocalization (n/CRHR1+)
CRHR1+
TH+
PV+
TH+/CRHR1+
PV+/CRHR1+

Figure S6. Single nucleus RNA sequencing (snRNA-Seq) using CRHR1-Cre::INTACT mice. (**A**) Scheme of workflow of snRNA-Seq in the ventral midbrain. (**B**) UMAP depicting 9 clusters of midbrain CRHR1 neurons, which can be specified into main clusters: dopaminergic (DA), glutamatergic (Glu) and GABAergic (GABA) CRHR1 neurons as well as oligodendrocytes (Oligo) and oligodendrocyte precursor cells (OPCs). (**C**) Violin plots depicting expression of marker genes for each cluster. (**D**) Distribution of marker genes for each cluster. (**E**) Number of cells belonging to different cell types. (**F**) GFP staining of nuclei of CRHR1 neurons in different brain regions of CRHR1-Cre::INTACT mice matching the expression pattern of endogenous CRHR1. (**G, H**) Co-staining of CRHR1 nuclei with markers of dopaminergic (TH) and GABAergic (PV) neurons in the SN. (**I**) Scheme illustrating the distribution of CRHR1 neurons within the SN and quantification of GABAergic and DAergic CRHR1 nuclei. (**J**) Distribution of DAergic and GABAergic CRHR1 neurons in the SN pars compacta (SNpc), and (**K**) in the SN pars reticulata (SNpr). Values represent mean ± SEM, scale bar = 200 µm.

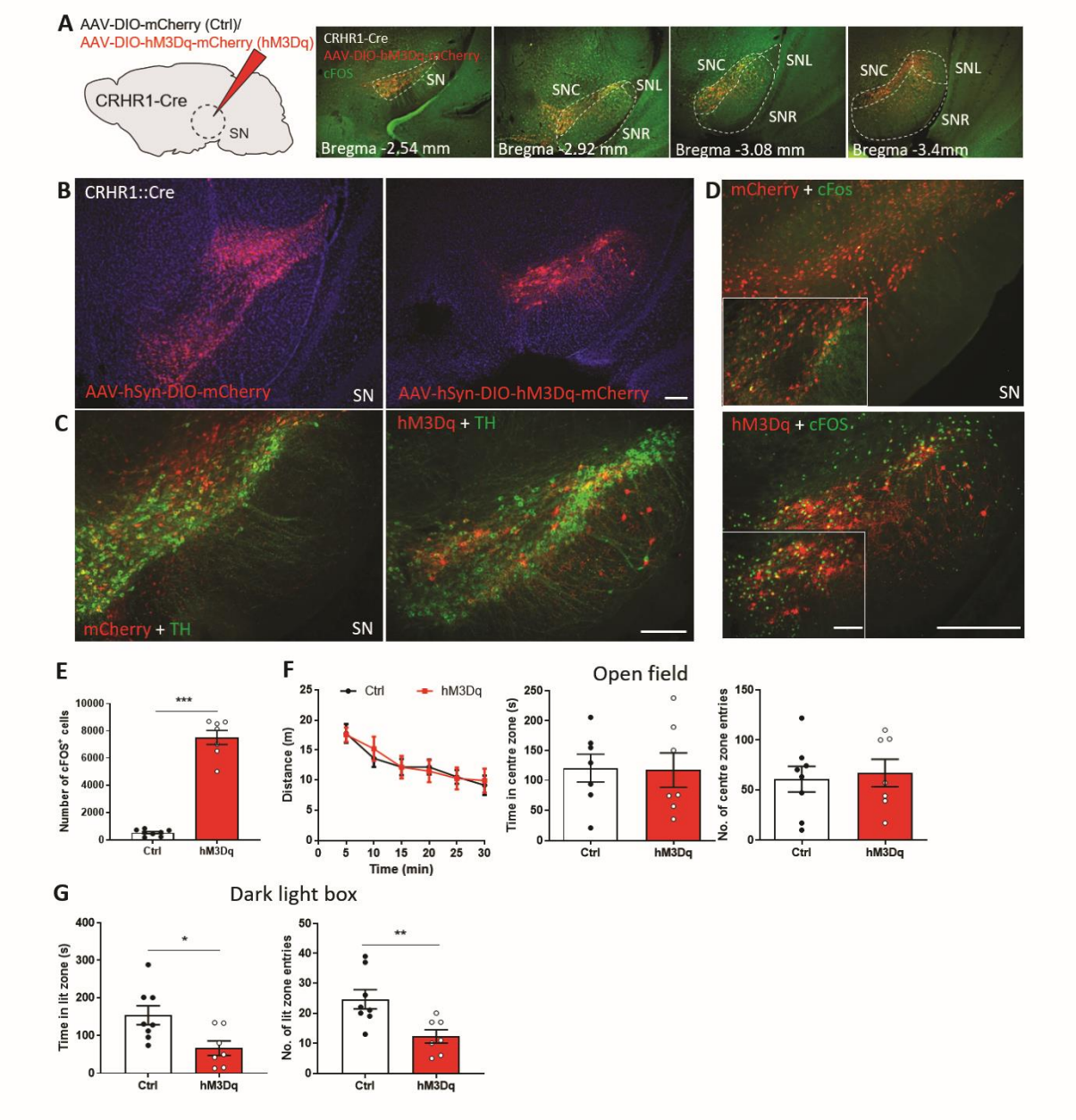

Figure S7. Stimulation of SN^{CRHR1} neurons does not affect locomotor activation. (**A**) Scheme illustrating the injection of AAV$_8$-hSyn-DIO-hM3Dq-mCherry or AAV$_8$-hSyn-DIO-mCherry into the SN of CRHR1-Cre mice and representative images of coronal sections showing the rostro-caudal spread of mCherry expression following virus injection. (**B**) Representative images showing mCherry distribution in the SN (**C**) combined with antibody staining against TH delineating the structure of the SN. (**D**) cFOS staining in the SN of CRHR1-Cre mice expressing hM3Dq. (**E**) Quantification of cFOS$^+$ cells in the SN ($p < 0.0001$, t = 11.73) 90 min following CNO administration. (**F**) Distance travelled (n = 8 (Ctrl), n = 7

(hM3Dq); $F_{1,14} = 0.01$, $p = 0.92$), time spent in the centre ($p = 0.93$, t = 0.08) and entries into the centre zone ($p = 0.74$, t = 0.33) of the open field. (**G**) Time spent in lit zone (n = 8 (Ctrl), n = 7 (hM3Dq); $p = 0.018$, t = 2.68) and entries into lit zone ($p = 0.008$, t = 3.09) of the dark-light box. Values represent mean ± SEM, * $p < 0.05$, ** $p < 0.01$, *** $p < 0.0001$, scale bar = 200 µm.

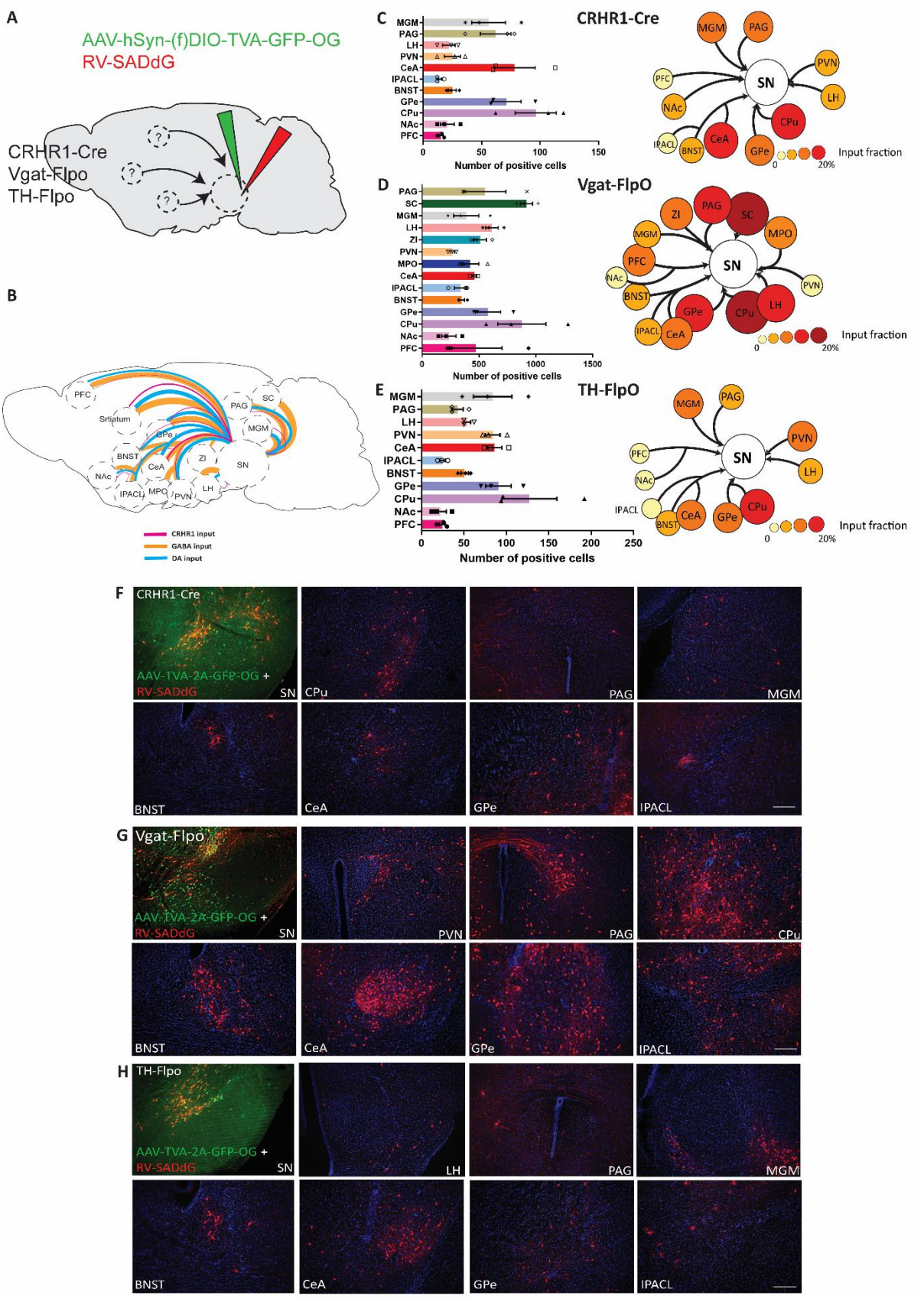

Figure S8. Rabies virus-based retrograde tracing reveals SN inputs. (**A**) Scheme depicting injection of AAV_1-CBh-DIO-TVA-2A-GFP-OG or AAV_1-CBh-fDIO-TVA-2A-GFP-OG and

RV-SADdG into the SN of CRHR1-Cre, Vgat-FlpO or TH-FlpO mice. (**B**) Summary of rabies virus tracing results using CRHR1-Cre, Vgat-FlpO, and TH-FlpO mice illustrating inputs to the SN from different brain regions. The strength of inputs is reflected by the thickness of the lines. Quantification (**C**-**E**) and representative images (**F**-**H**) of cells labelled by rabies virus-based retrograde tracing in different brain regions of CRHR1-Cre, Vgat-FlpO and TH-FlpO mice. Values represent mean ± SEM, scale bar = 200 μm. Abbreviations: CPu, caudate putamen; MGM, medial geniculate thalamic nucleus; SC, superior colliculus; ZI, zona incerta.

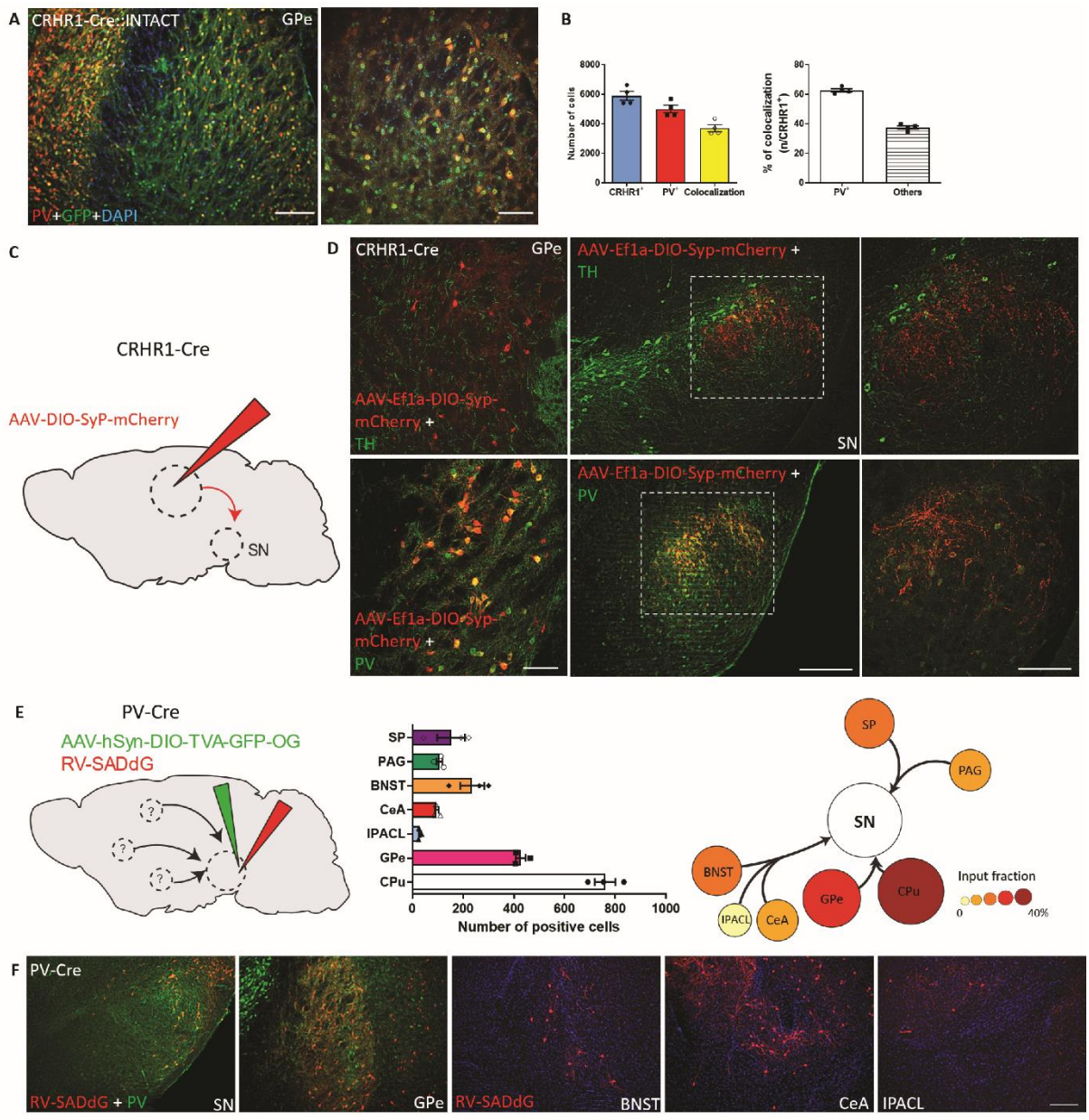

Figure S9. Characterization of GPe^{CRHR1} neurons. (**A**) Representative images showing nuclei of CRHR1 neurons in the GPe co-localizing with PV. (**B**) Quantification of CRHR1 and PV co-expression in the GPe. (**C**) Representative images of coronal GPe and SN section of CRHR1-Cre mice injected with AAV_8-DIO-Syp-mCherry into the GPe of CRHR1-Cre mice stained for TH and (**D**) PV. Higher magnification of marked area is shown to the left. (**E**) Representative images of coronal brain sections of the SN and retrogradely labelled brain regions. For retrograde tracing, AAV_1-CBh-DIO-TVA-2A-GFP-OG and RV-SADdG were

injected into the SN of PV-Cre mice. (**F**) Quantification of input neurons of SN^{PV} neurons throughout the brain. Values represent mean ± SEM, scale bar = 200 µm.

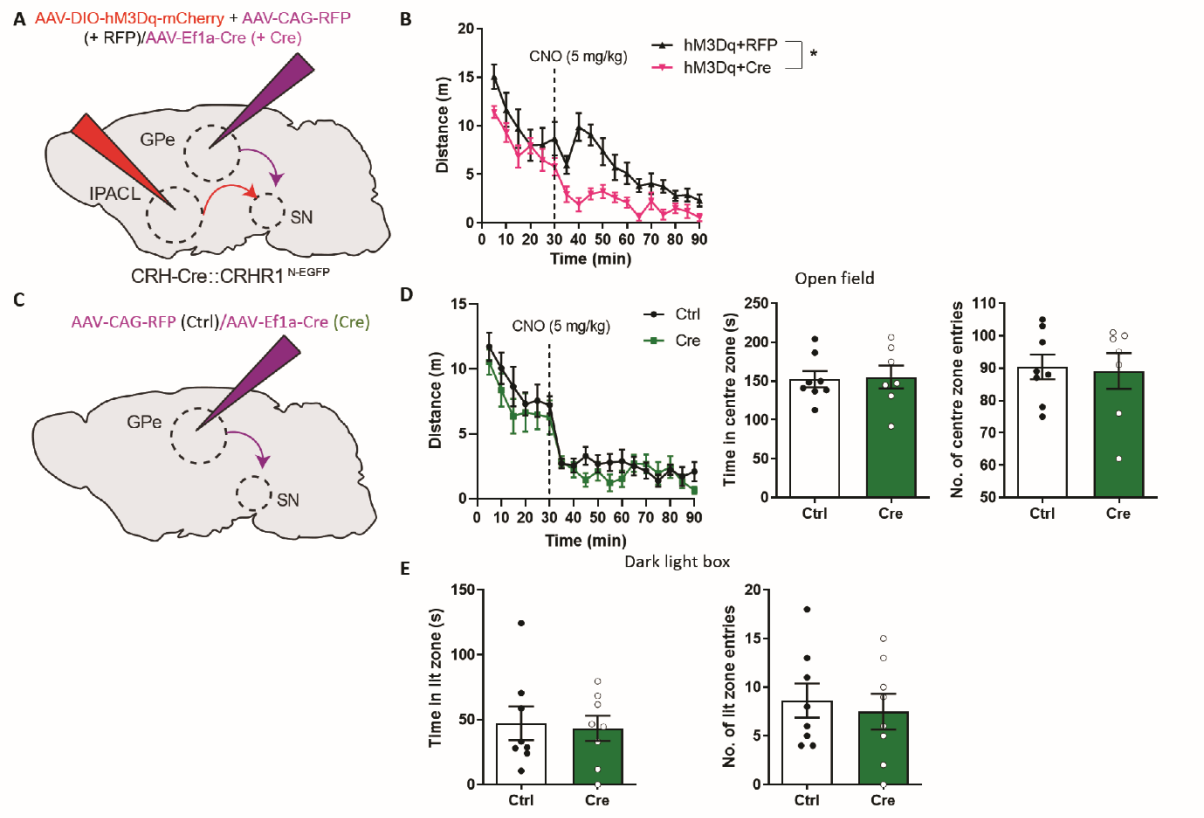

Figure S10. Assessing consequences of CRHR1 deletion from GPe^{CRHR1} neurons and respective control conditions. (**A**) Scheme illustrating injection of AAV_8-hSyn-DIO-hM3Dq-mCherry into the IPACL and of AAV_1-Ef1a-Cre (hM3Dq + Cre) or AAV_1-Ef1a-RFP (hM3Dq + Ctrl) into the GPe of CRH-Cre::CRHR1$^{N\text{-}EGFP}$ mice. (**B**) Locomotor activity of CRHR1-Cre mice injected with AAV_8-hSyn-DIO-hM3Dq (hM3Dq) or AAV_8-hSyn-DIO-mCherry (Ctrl) into the GPe in a 90-min open field test (n = 8 per group; repeated measures two-way ANOVA, $F_{1,16} = 7.4$, $p = 0.014$). (**C**) Schematic illustration of control experiment showing injection of AAV_1-Ef1a-Cre (Cre) or AAV_1-Ef1a-RFP (Ctrl) into the GPe of CRH-Cre::CRHR1$^{N\text{-}EGFP}$ mice. (**D**) Distance travelled (n = 8 per group; repeated measures two-way ANOVA, $F_{1,14} = 0.31$, $p = 0.58$), time spent in centre ($p = 0.86$, t = 0.18) and entries into the centre zone ($p = 0.86$, t = 0.19) of the open field. (**E**) Time spent in lit zone (n = 8 per group; $p = 0.8$, t = 0.25) and entries into lit zone ($p = 0.67$, t = 0.44) of the dark-light box. Values represent mean ± SEM, * $p < 0.05$.

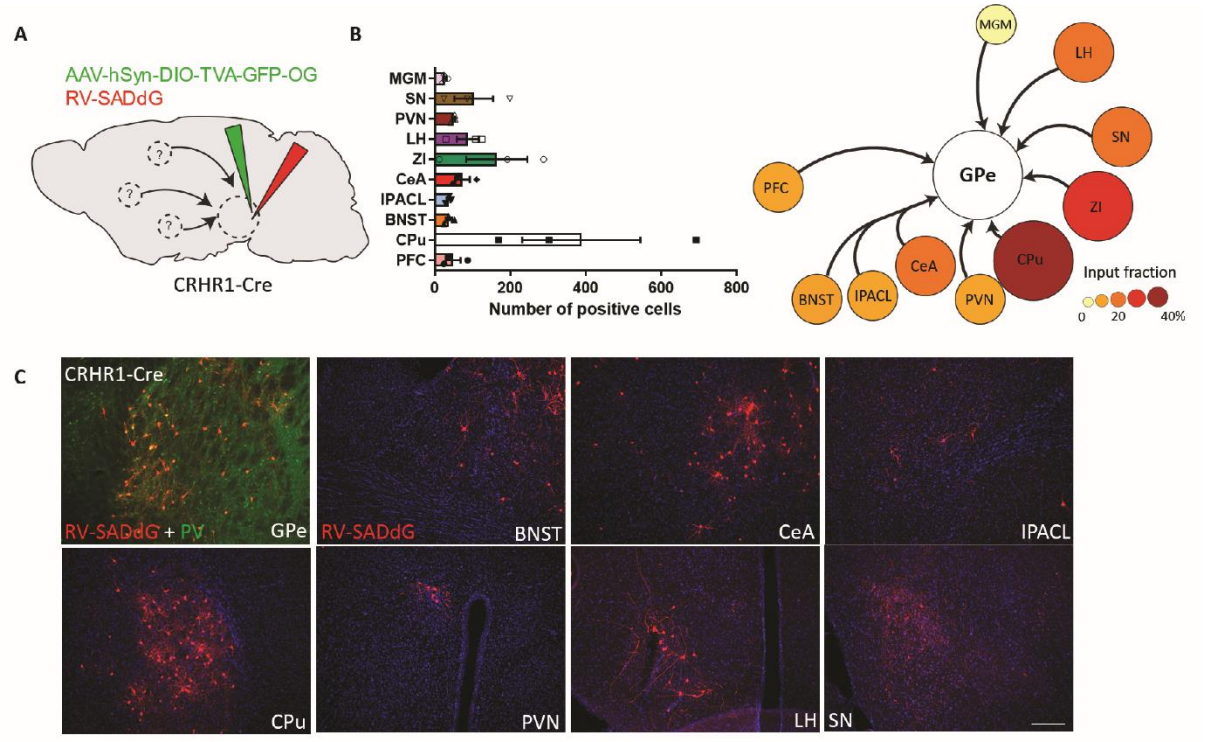

Figure S11. Rabies virus-based retrograde tracing reveals inputs of GPe^{CRHR1} neurons. (**A**) Scheme depicting injection of AAV$_1$-CBh-DIO-TVA-2A-GFP-OG and RV-SADdG into the GPe of CRHR1-Cre mice. Representative images of coronal brain sections of the GPe and retrogradely labelled brain regions. For retrograde tracing, AAV$_1$-CBh-DIO-TVA-2A-GFP-OG and RV-SADdG were injected into the SN of CRHR1-Cre mice. (**B**) Quantification of input neurons of GPe^{CRHR1} neurons throughout the brain. (**C**) Representative images of cells labelled by rabies virus-based retrograde tracing in different brain regions of CRHR1-Cre mice. Values represent mean ± SEM. All scale bars = 200µm.

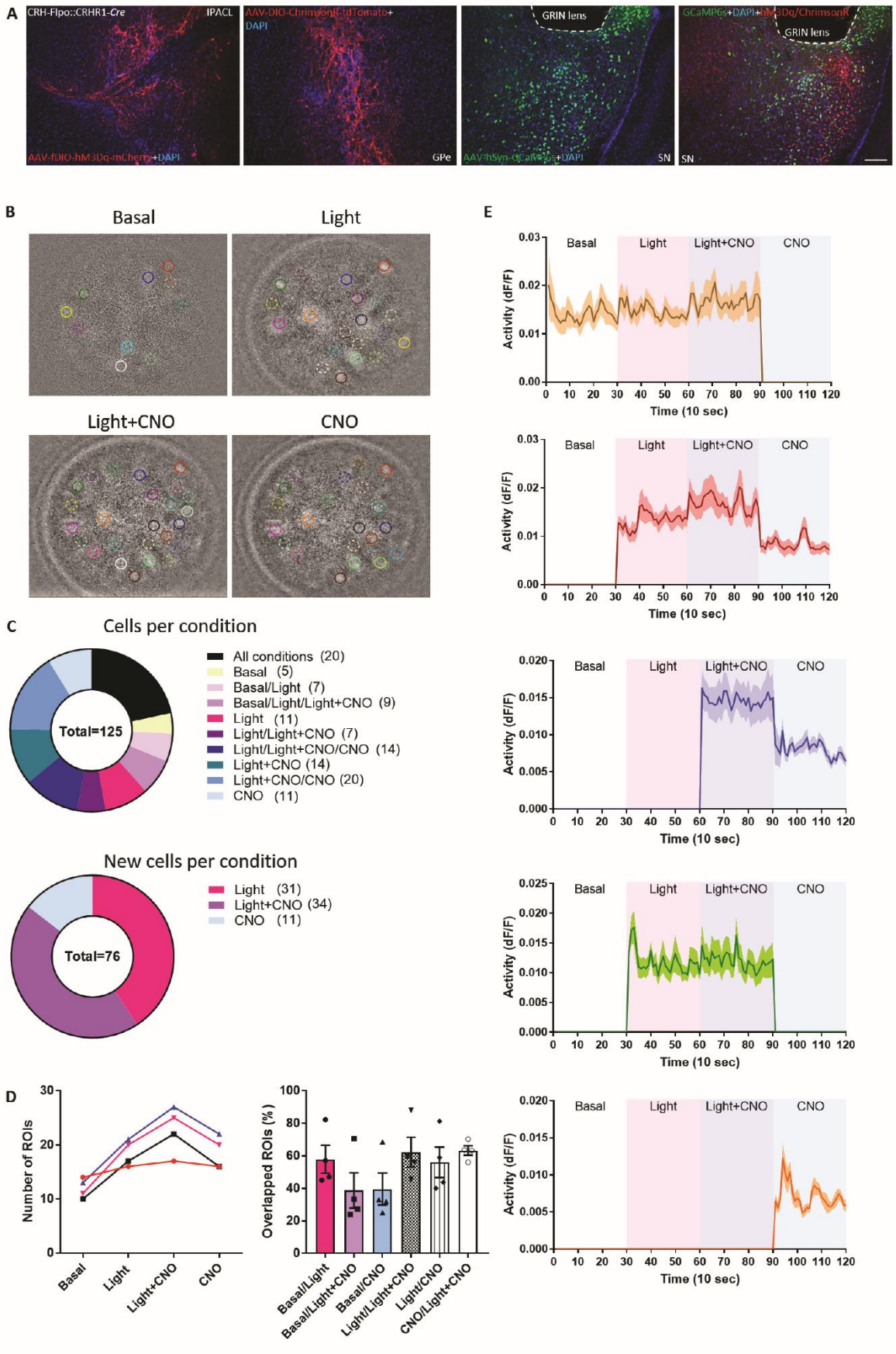
A
CRH-Flpo::CRHR1-Cre
IPACL
AAV-fDIO-hM3Dq-mCherry+DAPI
AAV-DIO-ChrimsonR-tdTomato+ DAPI
GPe
GRIN lens
AAV-hSyn-GCaMP6s+DAPI
SN
GCaMP6s+DAPI+hM3Dq/ChrimsonR
GRIN lens
SN
B
Basal
Light
Light+CNO
CNO
C
Cells per condition
Total=125
All conditions (20)
Basal (5)
Basal/Light (7)
Basal/Light/Light+CNO (9)
Light (11)
Light/Light+CNO (7)
Light/Light+CNO/CNO (14)
Light+CNO (14)
Light+CNO/CNO (20)
CNO (11)
New cells per condition
Total=76
Light (31)
Light+CNO (34)
CNO (11)
D
Number of ROIs
Basal
Light
Light+CNO
CNO
Overlapped ROIs (%)
Basal/Light
Basal/Light+CNO
Basal/CNO
Light/Light+CNO
Light/CNO
CNO/Light+CNO
E
Basal
Light
Light+CNO
CNO
Activity (dF/F)
Time (10 sec)

Figure S12. In vivo calcium imaging reveals differential cellular responses depending on stimulation conditions. (**A**) Representative images showing sites of virus injection and GRIN lens implantation in the lateral SN. (**B**) Representative images showing ROIs detected under different conditions during miniscope recording. (**C**) Pie charts showing the distribution of cells and number of newly appeared cells during different conditions. (**D**) Number of ROIs captured from each animal under different stimulation conditions. Number of overlapping ROIs under different stimulation conditions. (**E**) Traces of clusters of cells activated during different stimulation conditions. Values represent mean ± SEM, scale bar = 200 μm.

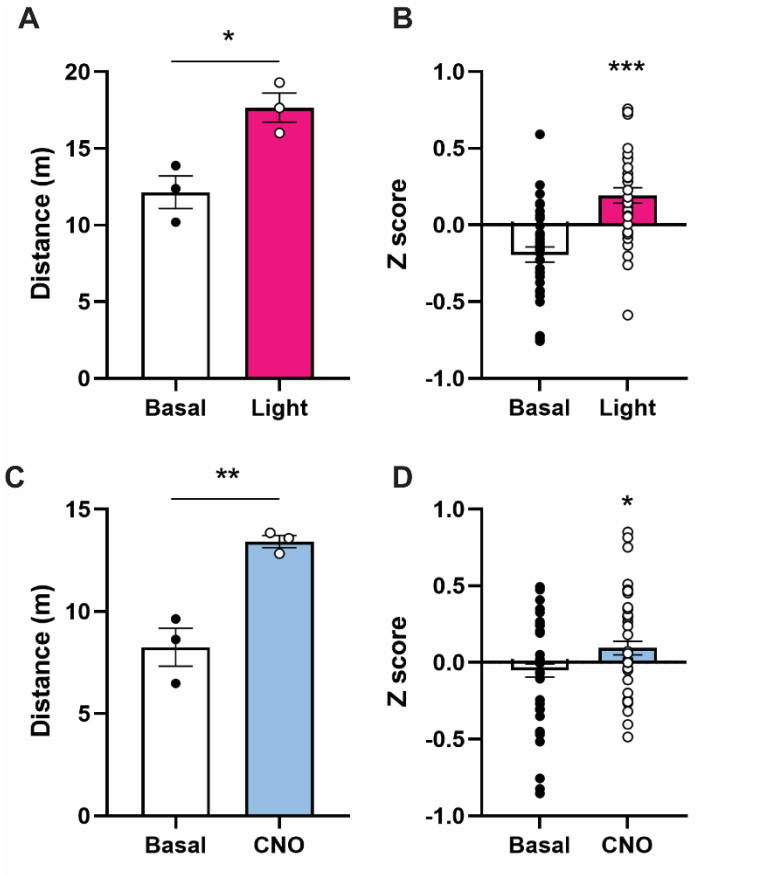

Figure S13. In vivo calcium imaging reveals differential cellular responses depending on stimulation conditions. (**A**) Distance mice travelled in the OF with 5 min basal condition and during 5 min light stimulation at GPe^{CRHR1} terminals in the SN (n = 3 animals; $p = 0.018$, t = 3.86). (**B**) Activation of GPe^{CRHR1} terminals increased local cell activities ($p < 0.0001$, t = 5.5). (**C**) CNO administration increased the distance mice travelled through activation of IPACL^{CRH} neurons. Basal = 0-5 min, CNO = 15-20 min following CNO administration (n = 3 animals per group; $p = 0.006$, t = 5.3). (**D**) Activation of IPACL^{CRH} neurons increased local cell activities ($p = 0.02$, t = 2.36). Values represent mean ± SEM, * $p < 0.05$, ** $p < 0.01$, *** $p < 0.0001$.

Movie S1. Brain clearing reveals distribution of CRH^+ neurons throughout the mouse brain. A CRH-Cre::Ai9 mouse brain was cleared using CLARITY revealing the distribution of CRH^+ neurons (white signals) across the brain. CRH^+ neurons are found at high density in regions of the extended amygdala.

Movie S2. Distribution of CRH^+ neurons in the extended amygdala. CLARITY on 1 mm-thick brain slice of CRH-Cre::Ai9 mouse demonstrates the spatial distribution of CRH^+ neurons (white signals) in the IPACL and CeA.

Movie S3. $IPACL^{CRH}$ neurons send projections to the SN. AAV-hSyn-DIO-mCherry was injected into the IPACL of CRH-Cre mice. Staining of mCherry (white signals) and CLARITY reveals $IPACL^{CRH}$ neurons and their projections to the SN.

Movie S4. Extended amygdala CRH^+ neurons project to the SN. CLARITY on CRH-Cre::Ai9 mouse brain shows CRH^+ neurons in the extended amygdala (white signals). Longer exposure times reveal details of projections to midbrain structures including the SN.

Movie S5. GPe^{CRHR1} neurons send direct projections into the SN. AAV-hSyn-DIO-mCherry was injected into the GPe of CRHR1-Cre mice. Staining of mCherry (white signals) and CLARITY reveals GPe^{CRHR1} neurons and their projections into the SN.